Cell, Vol. 86, 917–927, September 20, 1996, Copyright ©1996 by Cell Press

Anion Exchanger 1 (Band 3) Is Required to Prevent Erythrocyte Membrane Surface Loss but Not to Form the Membrane Skeleton

Luanne L. Peters,[1,2] Ramesh A. Shivdasani,[2,10] Shih-Chun Liu,[4] Manjit Hanspal,[4] Kathryn M. John,[2] Jennifer M. Gonzalez,[2] Carlo Brugnara,[5] Babette Gwynn,[1] Narla Mohandas,[6] Seth L. Alper,[7,8] Stuart H. Orkin,[2,3,9] and Samuel E. Lux[2,3,8]

[1]The Jackson Laboratory
Bar Harbor, Maine 04609
[2]Division of Hematology/Oncology
Department of Medicine
Children's Hospital
[3]Department of Pediatric Oncology
Dana-Farber Cancer Institute
Boston, Massachusetts 02115
[4]Department of Biomedical Research
St Elizabeth's Medical Center
Boston, Massachusetts 02115
[5]Department of Laboratory Medicine
Children's Hospital
Boston, Massachusetts 02115
[6]Lawrence Berkeley National Laboratory
University of California
Berkeley, California 94720
[7]Molecular Medicine and Renal Units
Department of Medicine
Beth Israel Hospital
[8]Department of Cell Biology
Harvard Medical School
Boston, Massachusetts 02115
[9]Howard Hughes Medical Institute
Children's Hospital
Boston, Massachusetts 02115

Summary

The red blood cell (RBC) membrane protein AE1 provides high affinity binding sites for the membrane skeleton, a structure critical to RBC integrity. AE1 biosynthesis is postulated to be required for terminal erythropoiesis and membrane skeleton assembly. We used targeted mutagenesis to assess AE1 function in vivo. RBCs lacking AE1 spontaneously shed membrane vesicles and tubules, leading to severe spherocytosis and hemolysis, but the levels of the major skeleton components, the synthesis of spectrin in mutant erythroblasts, and skeletal architecture are normal or nearly normal. The results indicate that AE1 does not regulate RBC membrane skeleton assembly in vivo but is essential for membrane stability. We postulate that stabilization is achieved through AE1–lipid interactions and that loss of these interactions is a key pathogenic event in hereditary spherocytosis.

Introduction

The RBC anion exchanger (AE1, band 3) is a major ($\sim 10^6$ copies per RBC) integral membrane protein composed of two structural domains that mediate its two distinct biological functions (Kopito and Lodish, 1985). The 60 kDa C-terminal domain consists of multiple hydrophobic segments that traverse the plasma membrane 12 to 14 times. The anion exchange activity of AE1 resides in this domain. The 43 kDa N-terminal domain has a net negative charge, projects into the cytoplasm, and mediates binding to the membrane skeleton components ankyrin, protein 4.1 and protein 4.2.

AE1 is one of a family of anion exchanger genes. In addition to RBCs, it is expressed in both mouse and human kidney as an alternative isoform that utilizes a downstream start codon and excludes exons 1 to 3 (Brosius et al., 1989). These exons encode amino acids involved in membrane skeleton binding (Willardson et al., 1989), and recent evidence confirms that this function is lacking in the truncated kidney isoform (Ding et al., 1994; Wang et al., 1995). AE2 is ubiquitously expressed but is especially prominent in the gastrointestinal tract and choroid plexus, while AE3 is expressed in brain neurons, the retina, heart, and kidney (reviewed in Alper, 1994). The membrane spanning domains of AE1, AE2, and AE3 are highly conserved and function in anion exchange. The cytoplasmic domains show less conservation; AE2 and AE3 have $\sim$300 additional amino acids at their N-termini (Alper, 1994).

AE1 is believed to be critical to the biosynthesis and mechanical properties of the RBC membrane through its association with the membrane skeleton, a multiprotein network lying just beneath and tethered to the plasma membrane (Lux and Palek, 1995). Spectrin, composed of tetramers of α and β subunits, is the major component of the membrane skeleton. Spectrin tetramers are cross-linked by short actin filaments at junctional complexes, which also include protein 4.1, myosin, tropomyosin, adducin, p55, and protein 4.9 (Gilligan and Bennett, 1993). The membrane skeleton is attached to the overlying plasma membrane at two sites. The major site is provided by the membrane skeleton protein ankyrin, which possesses high affinity binding sites for the cytoplasmic domain of AE1 and the β subunit of spectrin (Bennett and Stenbuck, 1979, 1980). The second attachment occurs at the junctional complexes, where protein 4.1 binds transmembrane glycophorin C (Reid et al., 1990). Ankyrin deficiency results in severe changes in RBC morphology and a markedly shortened RBC lifespan (Lux and Palek, 1995), whereas the absence of glycophorin C causes only a slight change in RBC morphology and survival (Chasis and Mohandas, 1992), suggesting that the glycophorin C–4.1 linkage is functionally less significant than the AE1–ankyrin–spectrin linkage. Protein 4.2, which binds ankyrin in vitro, may help stabilize the ankyrin–AE1 interaction (Korsgren and Cohen, 1988; Rybicki et al., 1988).

An intact membrane skeleton is crucial to the mechanical integrity of the RBC. The viscoelastic properties of the RBC, which allow it to withstand the shear forces of the circulation and squeeze through capillaries, are directly related to its spectrin content (Chasis et al., 1988; Waugh and Agre, 1988). Genetic defects in spectrin, or in proteins that attach the spectrin lattice to the

[10]Present address: Dana-Farber Cancer Institute, Boston, Massachusetts 02115.

bilayer (e.g., ankyrin, AE1, protein 4.1), result in loss of elasticity and deformability. Increased RBC fragility and cellular fragmentation ensue in humans and mice, producing abnormally shaped erythrocytes that are removed by the spleen. Severe and sometimes life-threatening hemolytic anemias result (Lux and Palek, 1995). They are classified by morphology as hereditary spherocytosis (HS), elliptocytosis (HE), or pyropoikilocytosis (HPP). HE and HPP result from "horizontal" membrane skeleton defects affecting protein 4.1 or the end-to-end association of α- and β-spectrin. HS is caused by loss of "vertical" connections attaching the skeleton to the overlying lipid bilayer. These involve α-spectrin, β-spectrin, ankyrin, protein 4.2, and AE1.

AE1 is thought to play a pivotal role in the assembly of the membrane skeleton in developing erythroblasts. In vitro evidence indicates that the proper spatial and temporal translocation of cytoplasmic membrane skeleton components into a stable supramolecular complex at the plasma membrane requires prelocalization of AE1 within the plasma membrane. Pulse-chase studies of metabolically labeled avian erythroid precursors (Woods et al., 1986; Cox et al., 1987; Lazarides, 1987) and murine erythroleukemia (MEL) cells (Hanspal and Palek, 1987; Lehnert and Lodish, 1988; Hanspal et al., 1992a, 1992b) reveal that spectrin and ankyrin are synthesized prior to AE1 in developing erythroblasts and constitute a labile cytoplasmic pool. Upon induction of AE1 synthesis, preassembled spectrin and ankyrin shift into the stable, membrane-bound fraction. Similar results are obtained in human erythroleukemia cells (Nehls et al., 1993). In normal human bone marrow erythroblasts, however, synchronous synthesis of AE1, spectrin, and ankyrin occurs (Nehls et al., 1993), suggesting that the sequential assembly hypothesis applies only to transformed cells.

In vitro studies of transformed avian erythroblasts also suggest that AE1 plays a role in RBC proliferation and terminal differentiation (Zenke et al., 1988). Proliferation of undifferentiated erythroblasts correlates with a reversible block in transcription and synthesis of AE1; changing the pH of the culture medium allows transcription and synthesis of AE1 to resume and, notably, RBC differentiation to proceed.

In humans no homozygous AE1 mutations have been identified (Lux and Palek, 1995), suggesting that homozygous AE1 deficiency is lethal. To address the role of AE1 in developing RBCs in vivo, we used gene targeting in embryonic stem (ES) cells to create a null mutation in mice. Here we have examined the hematological consequences of AE1 deficiency. Surprisingly, no fetal loss of homozygotes occurs and some survive to adulthood and are fertile. Remarkably, despite a severe hemolytic anemia, AE1 null RBCs possess normal levels of spectrin and protein 4.1 and near normal membrane skeleton architecture. Moreover, RBC differentiation proceeds to the mature, enucleate stage. Our findings indicate that localization of AE1 within the plasma membrane is not a prerequisite for proper membrane skeleton assembly or terminal RBC differentiation. Moreover, the presence of severe hemolytic anemia despite an intact membrane skeleton suggests that AE1 stabilizes membrane lipids and that membrane loss in hereditary spherocytosis results from loss of this function.

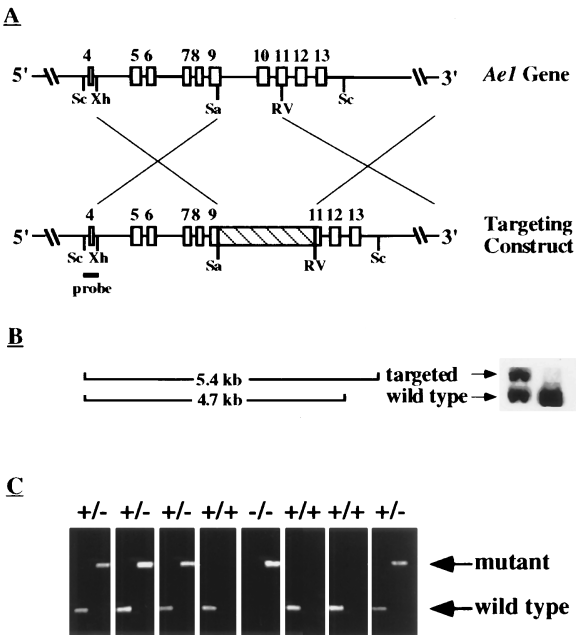

Figure 1. Targeted Disruption of the Murine *Ae1* Gene

(A) Partial restriction map of a portion of the *Ae1* locus with the targeting construct shown below. Numbered boxes represent exons. Upon homologous recombination in embryonic stem (ES) cells, a neomycin resistance (hatched box) cassette replaced a portion of exon 9, all of exon 10, part of exon 11, and the intervening introns. A 217 bp 5′ flanking SacI–XhoI fragment (black bar below exon 4) was used as the hybridization probe to distinguish alleles by Southern blot analysis. Sc, SacI; Xh, XhoI; Sa, SalI; and RV, EcoRV.

(B) Southern blot analysis of G418-resistant ES cell clones. Homologous recombination occurred in 2 of 89 clones, as indicated by the presence of both wild-type (4.7 kb) and targeted (5.4 kb) alleles in SacI digested DNA.

(C) Polymerase chain reaction analysis of offspring of an AE1$^{+/-}$ intercross reveals all three Mendelian genotypes: −/−, homozygous "knockouts"; +/−, heterozygotes; +/+, wild type.

Results

Targeted Disruption of the *Ae1* Gene

The mouse *Ae1* gene consists of 20 exons (Kopito et al., 1987). We replaced an 1130 base pair segment between exons 9 and 11 with a neoR cassette (Figure 1A). This segment encompasses the distal portion of the N-terminal cytoplasmic domain and the first membrane-spanning segment of the C-terminal domain.

Genotyping at birth reveals the expected Mendelian frequency (25.9%) of homozygous mutant (AE1$^{-/-}$) offspring from heterozygous (AE1$^{+/-}$) mating pairs (Figure 1C). No AE1 transcript is detected in newborn reticulocyte or 14.5-day fetal liver RNA using a full-length *Ae1* cDNA (Figure 2A). No protein is detected using antibodies raised against either the cytoplasmic or membrane-spanning domains of AE1 in RBC membranes (Figure 2B) or in whole cell lysates (data not shown), confirming the absence of the normal AE1 gene product as well as the absence of any truncated AE1 polypeptides derived from the targeted gene. Functional analysis of anion transport activity reveals that DIDS (4,4'-diisothiocyanostilbene-2,2'-disulfonate, a specific covalent inhibitor of AE1-mediated transport)-sensitive RBC sulfate influx

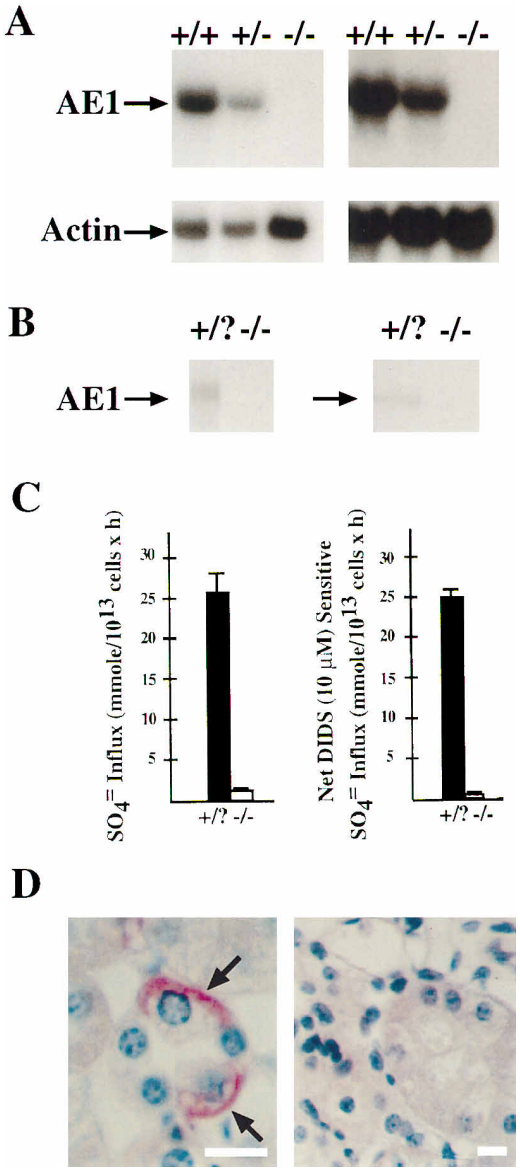

Figure 2. *Ae1* Gene Targeting Results in a Null Mutation

(A) Northern blot analyses of newborn reticulocyte (left) and 14.5-day fetal liver (right) RNA. Both filters were first probed with a full-length *Ae1* cDNA, then stripped and re-probed with an actin probe (Clonetech, Palo Alto, CA). *Ae1* mRNA (arrow, 3.4 kb) is absent in homozygous (−/−) mice. Hybridization intensity in heterozygous (+/−) reticulocytes and fetal liver RNA is reduced to ~50% of wild type (+/+).

(B) Immunoblot analysis of red blood cell (RBC) membranes (15 μg per lane) from newborn homozygotes (−/−) and normal littermates (+/?, designates data from phenotypically normal mice of +/+ and/or +/− genotype). The blots were probed with AE1 anti-peptide antibodies that recognize epitopes in the middle of the N-terminal cytoplasmic domain (left) and the C-terminal membrane-spanning domain (right). AE1 protein (arrow) is undetectable in −/− mice, even at 10× greater protein load (data not shown).

(C) Red blood cell anion transport. Sulfate influx in newborn homozygous (−/−) RBCs is dramatically decreased compared to normal littermates (+/?). AE1-independent influx (DIDS-insensitive) is minimal in both mutant and normal RBCs.

(D) Immunocytochemistry. AE1 protein, a basolateral marker of kidney type A intercalated cells, is detected in wild-type kidney (left, arrows) but not mutant kidney (right). Bar, 10 μm.

is reduced to 2.1% of normal in homozygotes (Figure 2C). Finally, type A intercalated cells are clearly present in AE1$^{-/-}$ kidney collecting ducts (S. L. A., unpublished data), but they contain no detectable AE1 (Figure 2D). Thus, the gene targeting produced a null mutation that disrupted both the RBC and kidney AE1 isoforms.

Hematological Analysis of AE1$^{-/-}$ Mice Reveals Severe Hemolytic Anemia

At birth AE1$^{-/-}$ mice are easily distinguished by their extreme pallor (Figure 3A). Although no fetal loss occurs, there is high mortality in the neonatal period: 85% of homozygotes die within the first two weeks. After that time the survival improves dramatically and the remaining 15% survive to adulthood. Adult AE1$^{-/-}$ mice are severely anemic and smaller than their normal littermates (Figure 3B). RBC counts, mean corpuscular volume (MCV), hemoglobin content (Hgb), and hematocrit (Hct) are dramatically decreased in newborn AE1$^{-/-}$ mice (Table 1). RBC volume and RBC hemoglobin concentration histograms reveal significant populations of microcytic and dehydrated cells (Figure 3C). The reticulocyte percentage is increased more than 2-fold and the spleen size is approximately twice normal (Table 1), indicating a compensatory increase in erythropoiesis. Adult AE1$^{-/-}$ mice show evidence of even more markedly accelerated erythropoiesis, perhaps explaining the improved survival rate following the first two weeks of life. AE1$^{-/-}$ adult spleens are more than 15 times the size of normal littermate spleens (7.7% ± 2.7% versus 0.45% ± 0.07% percent of body weight) with predominantly erythroid cells (data not shown). Reticulocyte counts are also elevated in adult AE1$^{-/-}$ mice (56.8% ± 12.2%) compared with normal sibs (2.1% ± 0.4%). As a result, adult AE1$^{-/-}$ mice maintain an average hematocrit of 18.1% ± 1.5% (versus 48.0% ± 1.3% in normal littermates). Mean spleen size, reticulocyte percentage, and hematocrits in adult AE1$^{+/-}$ mice do not differ from wild type (data not shown). However, they do show reduced DIDS-sensitive sulfate influx (68% of wild type, data not shown).

RBC morphology is markedly abnormal in AE1$^{-/-}$ mice. Striking microcytosis, spherocytosis, polychromatophilia, hyperchromasia, and poikilocytosis are seen on peripheral blood smears (Figure 3E). Scanning electron photomicrographs further reveal frequent rod-like membrane extensions that are often highly coiled (Figure 4E). Others are sinuously curved, suggesting they are flexible (not shown). The dramatic loss of membrane surface in AE1$^{-/-}$ RBCs and their markedly spherocytic shape are confirmed by osmotic gradient ektacytometry (Figure 3F). The DI_{max}, a measure of surface area, is profoundly decreased, and the O_{min} is displaced to a much higher than normal osmolality, indicating a low surface area-to-volume ratio (i.e., spherocytosis).

AE1$^{+/-}$ RBCs are mostly biconcave discs (Figure 4B), but rare membrane extensions are seen (not shown). Osmotic gradient ektacytometry confirms that these cells have also lost some membrane surface and are more spherocytic than normal (Figure 3F).

White blood cell (WBC) counts and differentials are normal in AE1$^{-/-}$ mice (data not shown), while nucleated

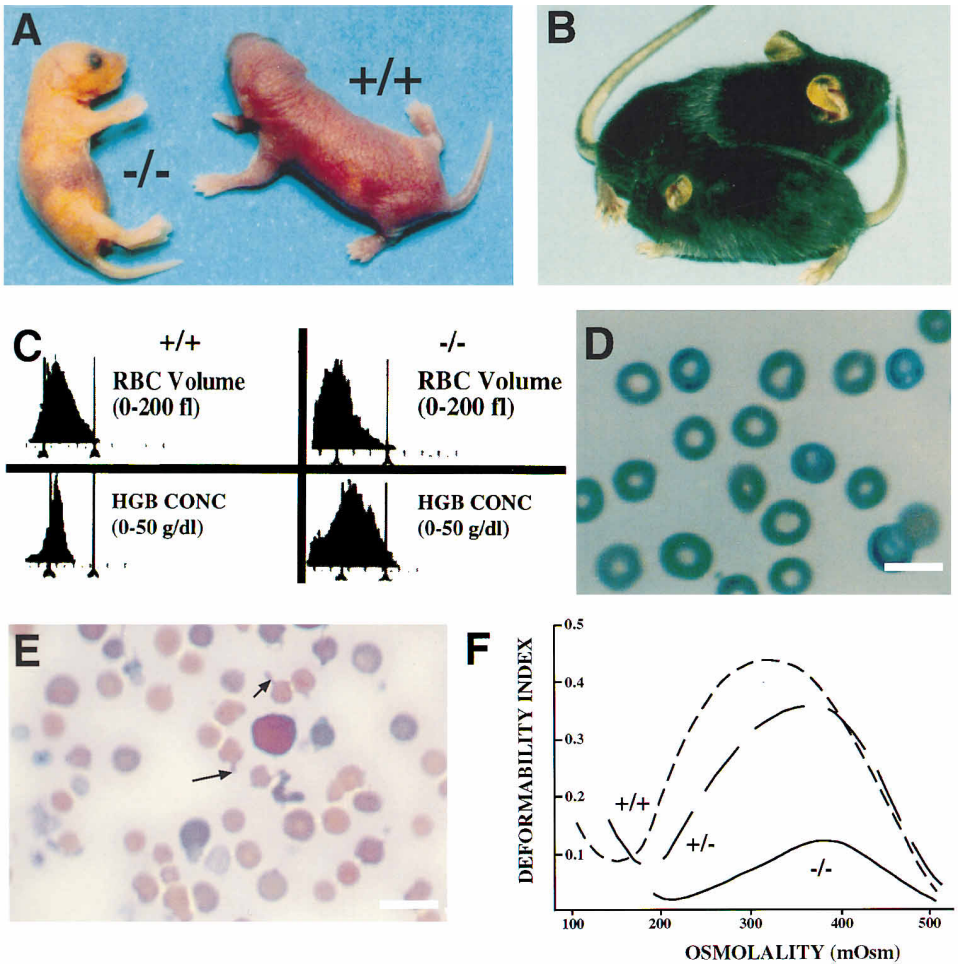

Figure 3. AE1-Deficient Mice Are Severely Anemic

(A) Appearance of a newborn mutant (−/−) mouse compared to a normal littermate (+/+).

(B) Appearance of an adult mutant (foreground) mouse compared to a normal littermate.

(C) RBC volume and hemoglobin concentration histograms of whole blood from normal (+/+) and mutant (−/−) newborn mice. Significant populations of small (upper panels) and dehydrated (bottom panels) RBCs are present in $AE1^{-/-}$ whole blood compared with controls.

(D) Wright's stained peripheral blood smear from a wild-type (+/+) newborn mouse. Bar, 10 μm.

(E) Wright's stained peripheral blood smears from a mutant (−/−) newborn mouse. Note the markedly abnormal and predominantly spherocytic RBC morphology. Long membrane extensions (arrows) are evident. Bar, 10 μm.

(F) Osmotic gradient ektacytometry. Representative osmotic deformability profiles of RBCs from a wild-type C57BL/6J newborn mouse (+/+) and heterozygous (+/−) and homozygous (−/−) AE1-deficient newborn mice. The maximum value of the deformability index (DI_{max}), a direct measure of RBC membrane surface area, is reduced in $AE1^{+/-}$ RBCs, and especially $AE1^{-/-}$ RBCs, quantitating the extraordinary loss of membrane surface material evident visually. The hypotonic osmolality at which the DI reaches a minimum (O_{min}) equals the osmolality at which 50% of RBCs lyse in a standard osmotic fragility test and correlates with RBC surface area-to-volume ratio. O_{min} is elevated in heterozygous and homozygous RBCs, confirming their spherocytic shape.

RBCs are elevated (171 per 100 WBCs versus 0 in normal littermates). $AE1^{-/-}$ blood smears also contain increased numbers of extruded nuclei ("smudge cells"). They are decreased by 91% when whole blood from $AE1^{-/-}$ mice is gently spread on a slide rather than smeared conventionally, suggesting the presence of a large population of mechanically fragile nucleated RBCs. Together, these data indicate that AE1 deficiency results in membrane

Table 1. Hematological Parameters in 5- to 7-Day Newborn Mice

Genotype	n	RBC ($\times 10^6/\mu l$)	Hgb (g/dl)	Hct (%)	MCV (fl)	Reticulocytes (%)	n	Spleen Weight (% Body Weight)	n
$AE1^{+/?}$	16	3.92 ± 0.06	9.9 ± 0.18	33.3 ± 0.40	85.2 ± 1.3	32.0 ± 1.9	12	0.63 ± 0.04	9
$AE1^{-/-}$	16	0.49 ± 0.10	2.0 ± 1.0	3.3 ± 0.07	69.3 ± 1.3	71.6 ± 2.1	7	1.14 ± 0.13	11

$AE1^{+/?}$ = normal littermate controls, $AE1^{-/-}$ = mutant. Hgb = hemoglobin, Hct = hematocrit, MCV = mean cell volume. All values represent mean ± standard error. By two tailed *t*-test, $p < 0.001$ for all determinations ($AE1^{+/?}$ vs. $AE1^{-/-}$) except spleen weight, where $p < 0.01$.

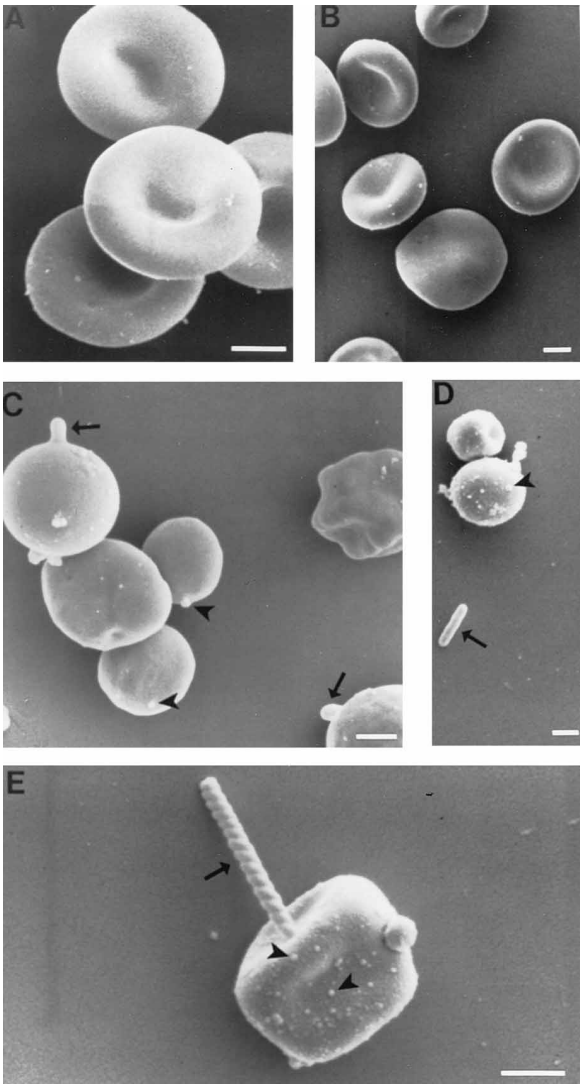

Figure 4. Scanning Electron Microscopy

RBCs from newborn wild-type (A), heterozygous (B), and AE1-deficient (C–E) mice. Note the markedly spherocytic shape of the AE1$^{-/-}$ RBCs. Many are shedding membrane vesicles (arrowheads). Others extrude rod-like membrane extensions (arrows), which are frequently detached (D, arrow). The membrane extensions often reach considerable length and are highly coiled (E). Adult mouse AE1$^{-/-}$ RBCs were morphologically indistinguishable. Bars, 1 μm.

loss (spherocytosis) and a severe hemolytic anemia, which is evident at birth and persists throughout life.

The Intrinsic Proliferative Capacity of AE1$^{-/-}$ Erythroid Precursors Is Normal

The accelerated erythropoiesis and presence of enucleated RBCs in AE1-null mice suggest that RBC proliferation and differentiation proceed in a manner responsive to the hemolytic stress. To confirm this, we performed in vitro erythroid colony assays. When mutant fetal liver cells are cultured in methylcellulose in the presence of erythropoietin and c-kit ligand, RBC numbers and morphology are indistinguishable from those of control littermates (54 ± 7 erythroid and mixed colonies per 10^5 plated cells). Further, the kinetics of colony formation do not appear to be perturbed (data not shown). Together with the in vivo findings, these results refute previous suggestions (Zenke et al., 1988) that AE1 is required for optimal RBC growth and differentiation.

AE1$^{-/-}$ RBCs Have Normal Spectrin Content

SDS–polyacrylamide gel electrophoresis (SDS–PAGE) analysis of Triton X-100 extracted RBC membranes reveals the membrane skeleton components α- and β-spectrin, ankyrin, actin, and protein 4.1 (Figure 5A). The spectrin–4.1–actin ratio in AE1$^{-/-}$ extracts is normal (1.0–0.9–1.3 versus 1.0–1.0–1.3 in normal controls). Western blot analyses confirm that immunoreactive spectrin, ankyrin, and protein 4.1 are present in AE1$^{-/-}$ RBC membranes (Figure 5B). However, protein 4.2 is not detectable in the membrane fraction or in whole cell lysates (Figure 5C) even when 5–10 times more AE1$^{-/-}$ protein than normal littermate protein is loaded onto the gel. In contrast, protein 4.2 RNA levels are normal in AE1$^{-/-}$ RBCs (data not shown). These data suggest that AE1 contributes a critical binding site for protein 4.2 within the membrane skeleton and that protein 4.2 is unstable in its absence.

Attempts to quantitate the absolute amounts of skeletal proteins in AE1$^{-/-}$ ghosts by gel and Western analyses are complicated by the fact that more hemoglobin is retained on membranes of AE1$^{-/-}$ RBCs during hypotonic lysis than on the membranes of normal RBCs (Figure 5D). Consequently, loading equal protein concentrations per well results in under-representation of the membrane skeleton fraction in AE1$^{-/-}$ samples. To overcome this difficulty we scanned SDS–PAGE gels to obtain the relative proportions of hemoglobin present in equal amounts of AE1$^{-/-}$, AE1$^{+/-}$ and wild-type RBC ghost preparations. When the integrated area representing each major membrane skeleton component is expressed as a percentage of the hemoglobin-free fraction, AE1$^{-/-}$ RBC ghosts contain 84.7% ± 5.5% (n = 10), 86.4% ± 5.4% (n = 10), and 48.8% ± 5.0% (n = 8) of wild-type, steady state levels of α-spectrin, β-spectrin, and ankyrin, respectively. The decrement in bound ankyrin seems appropriate in the absence of its major binding site on AE1. However, the near normal spectrin content in AE1-deficient RBC membranes is very surprising and suggests the possibility of alternative membrane binding sites for spectrin or alternative mechanisms of assembling the membrane skeleton. Similar analyses reveal normal amounts of α- and β-spectrin (94.8% ± 5.4% and 96.8% ± 4.2%, respectively, n = 6) and ankyrin (119% ± 6.9%, n = 5) but decreased levels of AE1 (82.3% ± 2.1%, n = 6) in AE1$^{+/-}$ RBCs.

The densitometric data were confirmed using two approaches to compensate for differences in membrane-bound hemoglobin. First, mutant and control membranes from 5×10^7 RBCs were compared by immunoblotting. Indeed, AE1$^{-/-}$ membranes contained normal quantities of α- and β-spectrin and protein 4.1, while ankyrin was decreased by ~50% (Figure 5B). Second, the synthesis, assembly, and turnover of spectrin and ankyrin were measured. In AE1$^{-/-}$ erythroblasts the soluble spectrin fraction, representing newly synthesized protein, is increased 1.5-fold compared to wild-type cells (Figure 5E). Moreover, the 2- to 3-fold excess

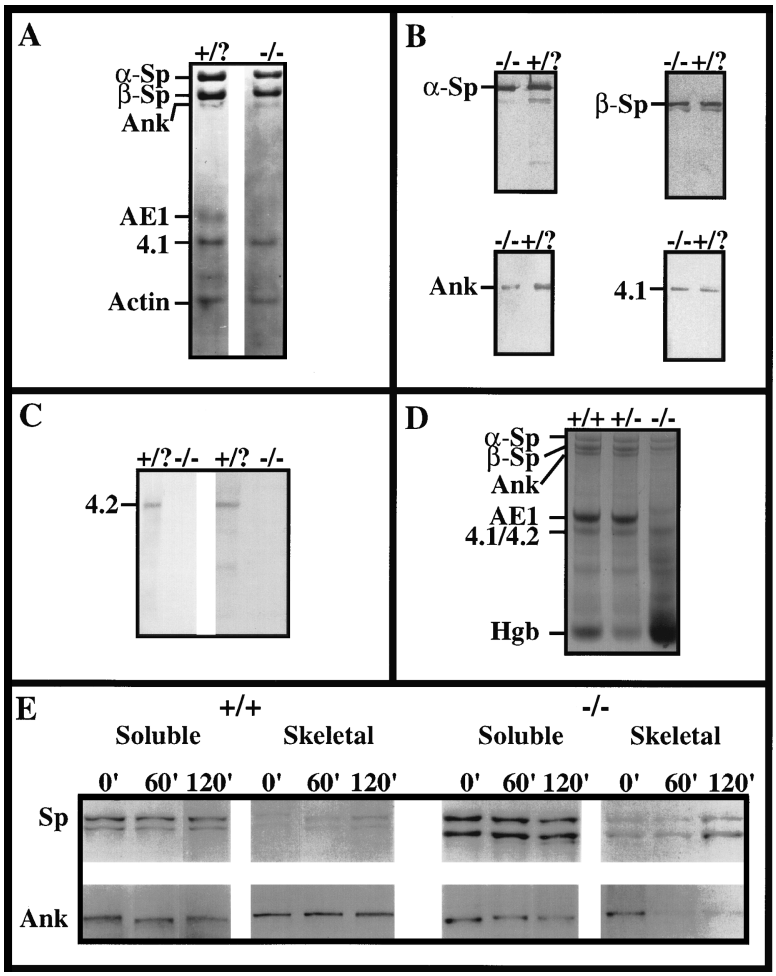

Figure 5. Membrane Skeleton in AE1-Deficient Mice

(A) Coomassie blue–stained SDS gel (Fairbanks buffer) of membrane skeletons from normal (+/?) and mutant (−/−) newborn mice. Note that AE1 is absent in AE1$^{-/-}$ skeletons but that all other membrane skeleton components are present. Similar results were obtained from adult mouse RBCs. Sp, spectrin; Ank, ankyrin.

(B) Western blots of α- and β-spectrin, ankyrin, and protein 4.1 in AE1-deficient (−/−) and normal (+/?) membranes prepared from 5×10^7 RBCs. Adult and newborn RBCs were analyzed and were similar.

(C) Western blots showing that protein 4.2 is absent in both RBC membranes (left) and whole cell lysates (right) from AE1-deficient (−/−) newborn mice (25 μg protein per lane). Adult AE1$^{-/-}$ RBCs showed similar 4.2 deficiency.

(D) Coomassie blue–stained SDS gel (Fairbanks buffer) of membrane protein from adult wild-type (+/+, 5 μg), heterozygous (+/−, 6 μg), and mutant (−/−, 8.5 μg) mouse RBCs. Note the increased hemoglobin (Hgb) in the mutant membrane fraction, resulting in an under-representation of the membrane skeleton components compared to control ghosts. Similar results were obtained from newborn mouse RBCs.

(E) Pulse–chase analysis of spectrin and ankyrin. Control (+/+) and AE1$^{-/-}$ (−/−) erythroblasts from adult mouse spleens were [^{35}S]methionine-labeled for 60 min; chased with unlabeled methionine for 0, 60, and 120 min; lysed; separated into soluble and skeletal fractions; and immunoprecipitated for spectrin (Sp) and ankyrin (Ank). The immunoprecipitates were analyzed by SDS–PAGE and fluorography. This experiment was performed three times with similar results. By scanning densitometry, spectrin incorporation into AE1$^{-/-}$ erythroblast membrane skeletons is 98% of normal at 120 min. However, the rate of spectrin incorporation is reduced compared with control erythroblasts; the proportion of counts incorporated at 0 and 60 min is 72% and 81%, respectively, of control. Ankyrin, although synthesized in normal amounts, is markedly reduced in AE1$^{-/-}$ erythroblast membrane skeleton fractions due to rapid turnover.

of newly synthesized α-spectrin compared to β-spectrin in wild-type RBCs is not seen in AE1$^{-/-}$ RBCs. Instead, the ratio is approximately 1:1 (Figure 5E). Such changes are characteristic of RBCs under increased erythropoietic drive, such as occurs in anemia (Hanspal et al., 1991) or during fetal erythropoiesis (Peters et al., 1992). Pulse–chase studies of metabolically labeled AE1$^{-/-}$ erythroblasts show that the newly incorporated spectrin turns over normally, resulting in normal amounts on the membrane. The proportion of total counts incorporated into AE1$^{-/-}$ erythroblast membrane skeletons after a 0, 60, and 120 min chase is 72%, 81%, and 98%, respectively, of wild type (Figure 5E). Thus, synthesis of the spectrin skeleton is delayed in AE1$^{-/-}$ erythroblasts but proceeds to completion. Similar studies show that ankyrin is synthesized in normal amounts in AE1$^{-/-}$ cells, but its assembly into the membrane skeleton is markedly reduced due to rapid turnover (Figure 5E). These results confirm the normal amount of spectrin and reduced amount of ankyrin in AE1$^{-/-}$ RBC membranes at steady state, described earlier.

AE1$^{-/-}$ RBCs Have Normal Membrane Skeleton Architecture

We conclude from the above studies that a membrane skeleton with normal spectrin, actin, and protein 4.1 content is assembled in the absence of AE1. To determine the physical correlate, we examined negatively stained, spread, RBC membrane skeletons by electron microscopy. Remarkably, the architecture of the skeleton is essentially normal in AE1$^{-/-}$ RBCs (Figures 6A and 6B). Junctional complexes, spectrin, and ankyrin are easily identified; their arrangement appears normal; and no evidence of membrane skeleton disruption (e.g., detached spectrin filaments) is discernible. In AE1$^{-/-}$ mice, the number of spectrin filaments per junctional complex (JC) is 4.60 ± 0.11 (n = 4, 120 JCs examined) compared to 5.14 ± 0.09 in AE1$^{+/+}$ mice (n = 3, 169 JCs examined). When the data are represented as JCs with specific numbers of spectrin filaments, AE1$^{-/-}$ mice have more JCs with 3 and 4 spectrin filaments attached, and less with 5 and 6, as compared to wild type (Figure 6C), accounting for the small but statistically significant ($p <$

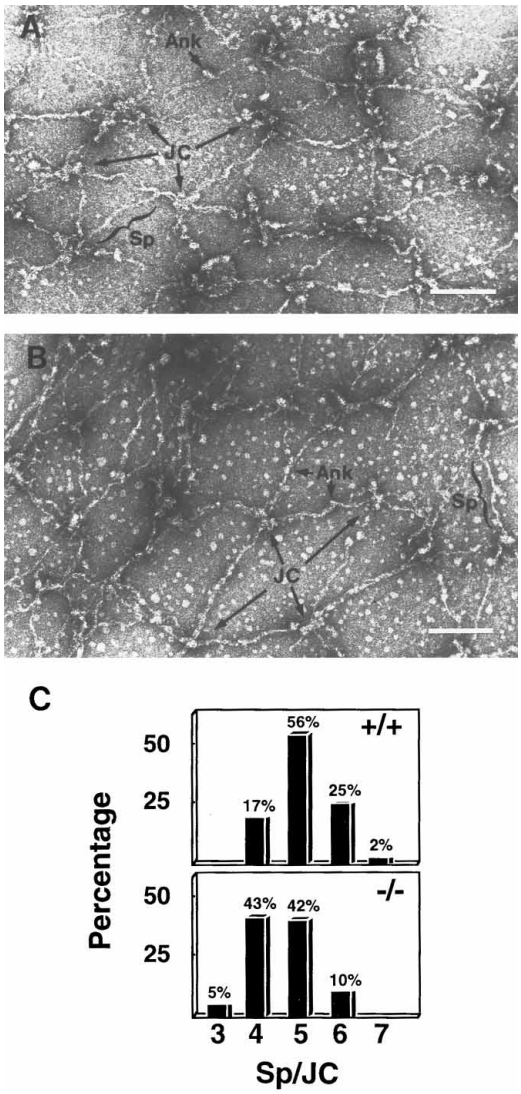

Figure 6. Ultrastructure of RBC Membrane Skeletons

(A and B) Negatively stained, spread membrane skeletons from RBCs of (A) control and (B) AE1-deficient (−/−) adult mice. Membrane skeletons of newborn mice are similar. Sp, spectrin filament; JC, junctional complexes; Ank, ankyrin. Bars, 100 nm.

(C) Quantitation of the number of spectrin filaments per junctional complex (Sp/JC) in adult wild-type (+/+) and mutant (−/−) membrane skeletons.

0.05, Student's two-tailed t test) overall decrease in the numbers of filaments per JC. These data are similar to those seen in asymptomatic human HPP carriers (Liu et al., 1990) and confirm that the RBC membrane skeleton is remarkably normal despite the absence of AE1.

Discussion

Biogenesis of the Membrane Skeleton

In vitro studies indicate that the major membrane skeleton components spectrin and ankyrin are synthesized before AE1 during RBC development and only bind to the membrane and form a membrane skeleton after AE1 synthesis begins (Cox et al., 1987; Lazarides, 1987; Hanspal et al., 1992a, 1992b). Our results call this model into question. Despite the complete absence of AE1 in targeted mice, an essentially normal membrane skeleton is present. Several observations contribute to this conclusion. The ratio of the major Triton X-100 insoluble membrane skeleton components (spectrin–protein 4.1–actin) is normal, indicating a lack of major disruptions to the structure. Electron microscopy reveals qualitatively normal membrane skeleton architecture and the number of spectrin filaments per junctional complex is only slightly reduced. Finally, pulse–chase studies reveal that spectrin is incorporated into the membrane skeleton of AE1$^{-/-}$ RBCs in normal amounts. It is noteworthy, however, that the temporal pattern of spectrin incorporation into the skeleton is altered in the absence of AE1, requiring 120 min of chase to reach normal control levels (Figure 5E).

The earlier studies indicating that stable membrane skeleton assembly is dependent upon AE1 insertion in the plasma membrane differ from those described here in that they utilized transformed avian erythroblasts or transformed murine erythroleukemia cells. Conceivably, these cells are inherently different from cells obtained directly from unperturbed erythropoietic compartments, as is the case in the present study. The synchronous synthesis of AE1, spectrin, and ankyrin observed by immunofluorescence in normal human bone marrow erythroblasts in situ (Nehls et al., 1993) supports this contention. Hence, other unknown factors must regulate membrane skeleton assembly in vivo.

An intact membrane skeleton in AE1-deficient RBCs suggests that additional spectrin attachment sites exist in the overlying plasma membrane. Recruitment of AE2 or AE3 does not occur, as no AE2 or AE3 expression is detected in AE1$^{-/-}$ erythroid tissues (data not shown). Two sites of attachment are well established, glycophorin C–4.1 linkages at the junctional complexes and AE1–ankyrin interactions (Lux and Palek, 1995). Direct association of spectrin with membrane lipids also occurs (Cohen et al., 1986; Maksymiw et al., 1987). In nonerythroid cells, repeat 1 of βII spectrin ("brain spectrin," or fodrin) and domain III of both βII spectrin and βIΣ2-spectrin ("muscle spectrin") contain functional, ankyrin-independent membrane protein binding domains, termed MAD1 (*m*embrane *a*ssociated *d*omain) and MAD2 (Lombardo et al., 1994). Perhaps erythroblasts contain spectrins with MAD1 or MAD2 domains or other alternative sites of attachment. Alternatively, the 4.1–glycophorin C and spectrin–lipid interactions may be sufficient to localize and orient the nascent membrane skeleton proteins and enable proper skeleton assembly. In addition, we cannot exclude the possibility that one or more of the many RBC integral membrane proteins other than AE1 are upregulated in AE1$^{-/-}$ RBCs and somehow compensate for the loss of AE1.

Recently, Inaba and colleagues (1996) have identified cattle that lack AE1 and protein 4.2 due to a nonsense mutation in the transmembrane domain of AE1. Surprisingly the animals have only moderate anemia and little evidence of hemolysis. The mutant RBC membranes also appear to be deficient in spectrin and actin; however, the spectrin analysis is limited to a single SDS–

PAGE gel and is not buttressed by immunostaining or biosynthetic studies, as in the present case. Electron microscopy of the inner membrane surface of the mutant RBCs shows decreased protein density, but the quick-freeze, deep-etch method used does not adequately resolve individual skeletal proteins to determine whether they are deficient or misaligned. Notably, humans with HS secondary to heterozygous AE1 deficiency have normal amounts of RBC spectrin (Reinhart et al., 1994; Jarolim et al., 1995), similar to the AE1-deficient mice.

Mice that are homozygous for the normoblastosis (*nb*) mutation have <1% of normal RBC ankyrin (reviewed in Peters and Lux, 1993). Like AE1$^{-/-}$ mice, they also have a severe spherocytic hemolytic anemia and normal RBC skeletal architecture (Liu et al., 1994). However, membrane vesiculation is much more prominent in AE1$^{-/-}$ RBCs. Membrane extensions, like the one pictured in Figure 4E, are not observed in *nb*/*nb* RBCs or in RBCs of spectrin-deficient mice (Peters and Lux, 1993). This suggests that AE1 is more important than ankyrin in stabilizing the RBC membrane and that loss of AE1 function is fundamental to the pathophysiology of HS.

Pathophysiology of Hereditary Spherocytosis

Two hypotheses exist regarding the mechanism of plasma membrane loss in HS (Lux and Palek, 1995). The first contends the lipid bilayer is primarily stabilized by interactions with the underlying spectrin skeleton. Spectrin-deficient areas would tend to bud off, leading to spherocytosis. The second argues the bilayer is primarily stabilized by interactions between lipids and the abundant AE1 molecules. Such interactions presumably spread beyond the first layer of lipids and influence the mobility of lipids in successive layers. In AE1-deficient red cells, this "lipid anchoring" function would be absent and unsupported lipids would tend to be lost, resulting in spherocytosis. Spectrin- and ankyrin-deficient red cells (Savvides et al., 1993) could also become spherocytic by this second mechanism. Since spectrin filaments corral AE1 molecules and limit their lateral movement (Sheetz et al., 1980), a decrease in spectrin would allow AE1's to diffuse and transiently cluster, fostering vesiculation.

Our data support the second hypothesis; severe membrane loss occurs in AE1 null RBCs in which the membrane skeleton is intact (Figure 6) and spectrin content is virtually normal (Figure 5). The coils, rods, and vesicles observed on the surface of AE1$^{-/-}$ RBCs (Figures 4C–4E) and detached in solution are morphologic evidence of this process. The membrane surface loss is confirmed by ektacytometry (Figure 3F). Proof of this hypothesis will require rescuing AE1$^{-/-}$ mice with portions of AE1 or chimeras of AE1 and other proteins, introduced as transgenes or by the "knock-in" approach.

Role of Protein 4.2 in the Membrane Skeleton

Inherited defects in the protein 4.2 gene cause hemolytic anemia in humans (Rybicki et al., 1988; Lux and Palek, 1995), yet its role in the RBC remains enigmatic. Although a 4.2–ankyrin complex can form in vitro (Korsgren and Cohen, 1988), no protein 4.2 is detected in AE1$^{-/-}$ RBCs, which retain 50% of the normal amount of ankyrin. It appears that AE1 contains the sole, high affinity binding site for protein 4.2. The total absence of protein 4.2 in RBCs of homozygous AE1-targeted mice raises the issue of its potential contribution to the mutant phenotype. In the absence of a mouse model of protein 4.2 deficiency, the impact of selective protein 4.2 deficiency in vivo, and its potential contribution to the phenotype of AE1$^{-/-}$ mice, will require an independent targeting of the protein 4.2 gene.

Future Issues

Targeted murine AE1 deficiency is remarkably similar to human HS, for which it provides a convenient and unique animal model. AE1-related human HS is manifest in the heterozygous state with a 15%–35% reduction in RBC AE1, mild hemolysis, mild spherocytosis, and little or no anemia (Jarolim et al., 1995; Lux and Palek, 1995). Heterozygous AE1-deficient mice show a similar subtle spherocytic (Figure 3F) phenotype, as described in the present study. Because mice survive homozygous AE1 deficiency, they present the opportunity to address outstanding questions regarding protein interactions within the mammalian RBC membrane skeleton and its association with the plasma membrane. Important examples include the link between AE1 and transmembrane glycophorins (Groves and Tanner, 1994), as well as alternate attachment sites for spectrin. In addition, the systemic acid–base ramifications of the absence of AE1 in kidney intercalated cells, the role of AE1 in establishing the RBC membrane potential, and the role of AE1 in other transport processes within the RBC can be addressed in AE1$^{-/-}$ mice. Rescue of AE1$^{-/-}$ RBCs with normal or modified AE1s will allow us to test a wide range of questions dealing with the structure and function of AE1, its involvement in RBC senescence (Kay et al., 1990), its reported lipid "flippase" activity (Ortwein et al., 1994; Vondenhof et al., 1994), and the mechanism of membrane lipid loss in HS.

Experimental Procedures

Targeted Disruption of the AE1 (Band 3) Gene

Genomic clones for murine AE1 were isolated from a 129/Sv lambda FixII library (Stratagene, La Jolla, CA). A 12.5 kb clone (mB3–10) extending from intron 1 to exon 20 (Kopito et al., 1987) was subcloned into the pPNT vector (Tybulewicz et al., 1991) to generate the targeting construct as follows (Figure 1A). A 2.1 kb XhoI–SalI fragment of mB3–10 was subcloned into the XbaI site of pPNT and a 6.6 kb fragment extending from an EcoRV site within exon 11 to an artificial SalI site within exon 20 was subcloned into the XhoI site of pPNT. Both fragments were oriented opposite the PGK-*neo*^{R} cassette of pPNT. Transfected J1 ES cells (Li et al., 1992) were cultured and selected in G418 and gancyclovir as described (Tybulewicz et al., 1991). Genomic DNA was analyzed by Southern blotting using a 217 base pair SacI–XhoI fragment as the probe. Blastocyst (C57BL/6J) injection and embryo transfer were performed using standard techniques (Robertson, 1987). Male chimeras, identified by coat color, were mated to C57BL/6J females to generate heterozygous mating pairs from which homozygous mutants (AE1$^{-/-}$) were obtained on a hybrid (129/Sv–C57BL/6J) inbred background.

Genotyping of Progeny by the Polymerase Chain Reaction

Genomic DNA was prepared from 3.0–4.0 mm tail samples and used to genotype progeny by polymerase chain reaction. For the detection of the wild-type allele, the oligonucleotides (5′ to 3′) AGGT ACACGGACAAGGTTTCTTGAT and AGGCCAGAGGGTTAGAGGTG

AATGTT were used as forward and reverse primers, respectively, and amplified a 400 bp fragment. The forward primer corresponds to a portion of the *Ae1* gene deleted by the targeting event; hence, the mutant allele was not amplified. The AE1 primer TTTTCTGGAGA AGCCTGTACTGGGCTT and *neo*^{R} primer GCCCGGTTCTTTTTGTC AAG amplified a 1300 bp fragment of the mutant allele.

Detection of Gene Products

Total RNA was isolated (Chomczynski and Sacchi, 1987) from fetal livers at 14.5 days gestation and from newborn reticulocytes, as described (Peters et al., 1993). For Northern blotting the probes were a 3.0 kb mouse *Ae1* cDNA encompassing the entire open reading frame (accession no. X02677), a 4.0 kb mouse *Ae2* cDNA (accession no. J04036), and a 4.0 kb human *AE3* cDNA (accession no. U05596).

Hemoglobin-depleted RBC membranes were prepared as described (Peters et al., 1995). Whole RBCs were dissolved in boiling electrophoresis sample buffer containing 10% SDS. Coomassie blue–stained gels (Laemmli, 1970; Fairbanks et al., 1971) were scanned with a Molecular Dynamics Computing Densitometer (Sunnyvale, CA). Immunoblots were performed as described (Peters et al., 1995), using rabbit polyclonal antibodies to spectrin (Lehnert and Lodish, 1988), ankyrin (Savvides et al., 1993), protein 4.1 (Jöns and Drenckhahn, 1992), and protein 4.2 (kindly provided by Dr. Carl M. Cohen, St Elizabeth's Medical Center, Boston, MA), or anti-peptide antibodies recognizing amino acids 214 to 228 (Alper et al., 1989) or the last 12 amino acids (Thomas et al., 1989) of mouse AE1.

Hematologic Analysis

Blood counts were determined using a Technicon H-3 instrument. Blood (50 μl) from newborn mice was collected in EDTA-coated microtiter tubes (Becton-Dickinson, Rutherford, NJ). Reticulocyte counts were determined by staining with new methylene blue (Sigma, St. Louis, MO).

In Vitro Proliferation Assays

Livers were harvested aseptically from fetuses 15–17 days postcoitus. Single cell suspensions were prepared by gentle disaggregation using a pasteur pipette. Cells were cultured in alpha medium supplemented with 0.9% methylcellulose (Stem Cell Technologies, Vancouver, BC, Canada), 30% fetal calf serum, 1% bovine serum albumin, 2 U/ml recombinant erythropoietin (Amgen, Thousand Oaks, CA), and 50 ng/ml recombinant c-kit ligand (Amgen) at densities of 1–5 $\times$ 10^5 cells per milliliter. Erythroid colonies were scored on the fifth and sixth days of culture.

Ultrastructural Studies

Scanning electron microscopy of RBCs was performed as described (Peters et al., 1992). For electron microscopy of membrane skeletons, ghosts were incubated on ice for 60 min in 1 mM sodium phosphate (pH 7.4) containing 2.5% Triton X-100 in a 1:1 ratio, and the intact skeletons were collected by centrifugation through a discontinuous gradient of 10% and 60% (wt/vol) sucrose, applied to carbon-coated grids, negatively stained with 1% uranyl acetate, and examined on a Jeol JEM-100 S electron microscope as described (Liu et al., 1987).

Biosynthesis Studies

AE1$^{-/-}$ spleens were placed in ice-cold Iscove's modified Dulbecco's medium (IMDM, GIBCO Laboratories, Grand Island, NY). Spleens were minced, passed through a 202 μm polyethylene mesh (Spectramesh, Spectrum Medical Industries, Los Angeles, CA) and applied to a discontinuous Percoll gradient (Pharmacia Fine Chemicals, Piscataway, NJ) consisting of 45%, 65%, 70%, 77%, and 90% Percoll in IMDM (Hanspal and Palek, 1987). Fraction 4 was almost entirely late (polychromatophilic and orthochromic) AE1$^{-/-}$ erythroblasts. Morphologically identical control erythroblasts were similarly obtained from spleens of BALB/c mice 25 days postinfection with Friend anemia virus (FVA) (Hanspal et al., 1992a). Control and AE1$^{-/-}$ erythroblasts were metabolically labeled with [^{35}S]methionine (30 μCi/ml, 1000 Ci/mmol, ICN Biomedicals, Irvine, CA) for 60 min, chased with unlabeled methionine (0.4 mM) for various time periods, lysed in buffered 1% Triton X-100, and separated into soluble and membrane skeleton fractions. Spectrin and ankyrin were immunoprecipitated using polyclonal antibodies as described (Hanspal et al., 1992a).

Other Studies

RBC sulfate transport (Schofield et al., 1992), immunocytochemical detection of AE1 in tissues (Peters et al., 1995), and osmotic gradient ektacytometry (Clark et al., 1983) were performed as described.

Acknowledgments

This work was supported by National Institutes of Health grants HL32262 (S. E. L.), DK34083 (S. E. L.), HL37462 (S.-C. L.), HL55321 (L. L. P.), HL27215 (M. H.), HL15157 (C. B.), DK26263 (N. M.), DK43495 (S. L. A.), and March of Dimes grant 5-FY94-0921 (L. L. P.). We thank S. L. Ciciotte, L. H. Derick, A. Stuart-Tilley, N. Magny, T. Nguyen, and M. Rosenblatt for technical assistance; S. Bean and M. Hogan for assistance with figures; and Drs. W. Beamer and P. Nishina for critically reviewing the manuscript.

Received June 18, 1996; revised July 31, 1996.

References

Alper, S.L. (1994). The band 3–related AE anion exchanger gene family. Cell Physiol. Biochem. *4*, 265–281.

Alper, S.L., Natale, J., Gluck, S., Lodish, H.F., and Brown, D. (1989). Subtypes of intercalated cells in rat kidney collecting duct defined by antibodies against erythroid band 3 and renal vacuolar H^+-ATPase. Proc. Natl. Acad. Sci. USA *86*, 5429–5433.

Bennett, V., and Stenbuck, P.J. (1979). Identification and partial purification of ankyrin, the high affinity membrane attachment site for human erythrocyte spectrin. J. Biol. Chem. *254*, 2533–2541.

Bennett, V., and Stenbuck, P.J. (1980). Association between ankyrin and the cytoplasmic domain of band 3 isolated from the human erythrocyte membrane. J. Biol. Chem. *255*, 6424–6432.

Brosius, F.C., III, Alper, S.L., Garcia. A.M., and Lodish, H.F. (1989). The major kidney band 3 transcript predicts an aminoterminal truncated band 3 polypeptide. J. Biol. Chem. *264*, 7784–7787.

Chasis, J.A., and Mohandas, M. (1992). Red blood cell glycophorins. Blood *80*, 1869–1879.

Chasis, J.A., Agre, P.A., and Mohandas, N. (1988). Decreased membrane mechanical stability and in vivo loss of surface area reflect spectrin deficiencies in hereditary spherocytosis. J. Clin. Invest. *82*, 617–623.

Chomczynski, P., and Sacchi, N. (1987). Single-step method of RNA isolation by acid guanidinium thiocyanate-phenol-chloroform extraction. Anal. Biochem. *162*, 156–159.

Clark, M.R., Mohandas, N., and Shohet, S.B. (1983). Osmotic gradient ektacytometry: comprehensive characterization of red cell volume and surface maintenance. Blood *61*, 899–910.

Cohen, A.M., Liu, S.-C., Derick, L.H., and Palek, J. (1986). Ultrastructural studies of the interaction of spectrin with phosphatidylserine liposomes. Blood *68*, 920–926.

Cox, J.V., Stack, J.H., and Lazarides, E. (1987). Erythroid anion transporter assembly is mediated by a developmentally regulated recruitment onto a preassembled membrane cytoskeleton. J. Cell Biol. *105*, 1405–1416.

Ding, Y., Casey, J.R., and Kopito, R.R. (1994). The major kidney AE1 isoform does not bind ankyrin (ANK1) in vitro. An essential role for the 79 NH_2-terminal amino acid residues of band 3. J. Biol. Chem. *269*, 32201–32208.

Fairbanks, G., Steck, T.L., and Wallach, D.F.H. (1971). Electrophoretic analysis of the major polypeptides of the human erythrocyte membrane. Biochemistry *10*, 2606–2617.

Gilligan, D.M., and Bennett, V. (1993). The junctional complex of the membrane skeleton. Semin. Hematol. *30*, 74–83.

Groves, J.D., and Tanner, M.J.A. (1994). The effects of glycophorin

A on the expression of the human red cell anion transporter (band 3) in Xenopus oocytes. J. Membr. Biol. *140*, 81–88.

Hanspal, M., and Palek, J. (1987). Synthesis and assembly of membrane skeletal proteins in mammalian red cell precursors. J. Cell Biol. *105*, 1417–1424.

Hanspal, M., Kalraiya, R., and Hanspal, J. (1991). Erythropoietin enhances the assembly of $\alpha\beta$ spectrin heterodimers on the murine erythroblast membranes by increasing β spectrin synthesis. J. Biol. Chem. *266*, 15626–15630.

Hanspal, M., Hanspal, J.S., Kalraiya, R., Liu, S.-C., Sahr, K.E., Howard, D., and Palek, J. (1992a). Asynchronous synthesis of membrane skeletal proteins during terminal maturation of murine erythroblasts. Blood *80*, 530–539.

Hanspal, M., Hanspal, J.S., Kalraiya, R., and Palek. J. (1992b). The expression and synthesis of the band 3 protein initiates the formation of a stable membrane skeleton in murine Rauscher-transformed erythroid cells. Eur. J. Cell Biol. *58*, 313–318.

Inaba, M., Yawata, A., Koshino, I., Sato, K., Takeuchi, M., Takakuwa, Y., Manno, S., Yawata, Y., Kanazaki, A., Sakai, J., et al. (1996). Defective anion transport and marked spherocytosis with membrane instability caused by hereditary total deficiency of red cell band 3 in cattle due to a nonsense mutation. J. Clin. Invest. *97*, 1804–1817.

Jarolim, P., Rubin, H.L., Brabec, V., Chrobak, L., Zolotarev, A.S., Alper, S.L., Brugnara, C., Wichterle, H., and Palek, J. (1995). Mutations of conserved arginines in the membrane domain of erythroid band 3 lead to a decrease in membrane-associated band 3 and to the phenotype of hereditary spherocytosis. Blood *85*, 634–640.

Jöns, T., and Drenckhahn, D. (1992). Identification of the binding interface involved in linkage of cytoskeletal protein 4.1 to the erythrocyte anion exchanger. EMBO J. *11*, 2863–2867.

Kay, M.M.B., Marchalonis, J.J., Hughes, J., Watanabe, K., and Schluter, S.F. (1990). Definition of a physiologic aging autoantigen by using synthetic peptides of membrane protein band 3: localization of the active antigenic sites. Proc. Natl. Acad. Sci. USA *87*, 5734–5738.

Kopito, R.R., and Lodish, H.F. (1985). Primary structure and transmembrane orientation of the murine anion exchange protein. Nature *316*, 234–238.

Kopito, R.R., Andersson, M., and Lodish, H.F. (1987). Structure and organization of the murine band 3 gene. J. Biol. Chem. *262*, 8035–8040.

Korsgren, C., and Cohen, C.M. (1988). Associations of human erythrocyte protein 4.2. Binding to ankyrin and to the cytoplasmic domain of band 3. J. Biol. Chem. *263*, 10212–10218.

Laemmli, U.K. (1970). Cleavage of structural proteins during the assembly of the head of bacteriophage T4. Nature *227*, 680–685.

Lazarides, E. (1987). From genes to structural morphogenesis: the genesis and epigenesis of a red blood cell. Cell *51*, 345–356.

Lehnert, M.E., and Lodish, H.F. (1988). Unequal synthesis and differential degradation of alpha and beta spectrin during murine erythroid differentiation. J. Cell Biol. *107*, 413–426.

Li, E., Bestor, T.H., and Jaenisch, R. (1992). Targeted mutations of the DNA methyltransferase gene results in embryonic lethality. Cell *69*, 915–926.

Liu, S.-C., Derick, L.H., and Palek, J. (1987). Visualization of the hexagonal lattice in the erythrocyte membrane skeleton. J. Cell Biol. *104*, 527–536.

Liu, S.-C., Derick, L.H., Agre, P., and Palek, J. (1990). Alteration of the erythrocyte membrane skeletal ultrastructure in hereditary spherocytosis, hereditary elliptocytosis, and pyropoikilocytosis. Blood *76*, 198–205.

Liu, S.-C., Yi, S.J., Derick, L.H., Murray, J., Barker, J.E., Cho, M.R., Golan, D.E., and Palek, J. (1994). Assembly of band 3 and spectrin in the red cell membrane of ankyrin-deficient nb/nb mice. Blood (Suppl. 1) *84*, 362a.

Lombardo, C.R., Weed, S.A., Kennedy, S.P., Forget, B.G., and Morrow, J.S. (1994). βII-spectrin (fodrin) and $\beta I\Sigma 2$-spectrin (muscle) contain NH_2- and COOH-terminal membrane association domains (MAD1 and MAD2). J. Biol. Chem. *269*, 29212–29219.

Lux, S.E., and Palek, J. (1995). Disorders of the red cell membrane. In Blood: Principles and Practice of Hematology, R.I. Handin, S.E. Lux, T.P. Stossel, eds. (Philadelphia: JB Lippincott Co.), pp. 1701–1818.

Maksymiw, R., Sui, S.-F., Gaub, H., and Sackmann, E. (1987). Electrostatic coupling of spectrin dimers to phosphatidylserine containing lipid lamellae. Biochemistry *26*, 2983–2990.

Nehls, V., Zeitler-Zapf, P., and Drenckhahn, D. (1993). Different sequences of expression of band 3, spectrin, and ankyrin during normal erythropoiesis and erythroleukemia. Am. J. Pathol. *142*, 1565–1573.

Ortwein, R., Oslender-Kohnen, A., and Deuticke, B. (1994). Band 3, the anion exchanger of the erythrocyte membrane, is also a flippase. Biochim. Biophys. Acta *1191*, 317–323.

Peters, L.L., and Lux, S.E. (1993). Ankyrins: structure and function in normal cells and hereditary spherocytes. Semin. Hematol. *30*, 85–118.

Peters, L.L., Birkenmeier, C.S., and Barker, J.E. (1992). Fetal compensation of hemolytic anemia in mice homozygous for the normoblastosis, *nb*, mutation. Blood *80*, 2122–2127.

Peters, L.L., White, R.A., Birkenmeier, C.S., Bloom, M.L., Lux, S.E., and Barker, J.E. (1992). Changes in cytoskeletal mRNA expression and protein synthesis during murine erythropoiesis in vivo. Proc. Natl. Acad. Sci. USA *89*, 5749–5753.

Peters, L.L., Turtzo, C., Birkenmeier, C.S., and Barker, J.E. (1993). Distinct fetal *Ank-1* and *Ank-2* related proteins and mRNAs in normal and *nb/nb* mice. Blood *81*, 2144–2149.

Peters, L.L., John, K.M., Lu, F.M., Eicher, E.M., Higgins, A., Yialamas, M., Turtzo, L.C., Otsuka, A.J., and Lux, S.E. (1995). *Ank3* (epithelial ankyrin), a widely distributed new member of the ankyrin gene family and the major ankyrin in kidney, is expressed in alternatively spliced forms, including forms that lack the repeat domain. J. Cell Biol. *130*, 313–330.

Reid, M.E., Takakuwa, Y., Conboy, J.G., Tchernia, G., and Mohandas, N. (1990). Glycophorin C content of human erythrocyte membrane is regulated by protein 4.1. Blood *75*, 2229–2234.

Reinhart, W.H., Wyss, E.J., Arnold, D., and Ott, P. (1994). Hereditary spherocytosis associated with protein band 3 defect in a Swiss kindred. Brit. J. Haematol. *86*, 147–155.

Robertson, E.J. (1987). Teratocarcinomas and Embryonic Stem Cells: A Practical Approach (Oxford: IRL Press).

Rybicki, A.C., Heath, R., Wolf, J.L., Lubin, B., and Schwartz, R.S. (1988). Deficiency of protein 4.2 in erythrocytes from a patient with a Coombs negative hemolytic anemia. Evidence for a role of protein 4.2 in stabilizing ankyrin on the membrane. J. Clin. Invest. *81*, 893–901.

Savvides, P., Shalev, O., John, K.M., and Lux, S.E. (1993). Combined spectrin and ankyrin deficiency is common in autosomal dominant hereditary spherocytosis. Blood *82*, 2953–2960.

Schofield, A.E., Rearden, D.M., and Tanner, M.J.A. (1992). Defective anion transport activity of the abnormal band 3 in hereditary ovalocytic red cells. Nature *335*, 836–838.

Sheetz, M.P., Schindler, M., and Koppel, D.E. (1980). Lateral mobility of integral membrane proteins is increased in spherocytic erythrocytes. Nature *285*, 510–511.

Thomas, H.A., Machen, T.E., Smolka, A., Baron, R., and Kopito, R.R. (1989). Identification of a 185-kDa band 3-related polypeptide in oxyntic cells. Am. J. Physiol. *257*, C537–C544.

Tybulewicz, V.L.J., Crawford, C.E., Jackson, P.K., Bronson, R.T., and Mulligan, R.C. (1991). Neonatal lethality and lymphopenia in mice with a homozygous disruption of the *c-abl* proto-oncogene. Cell *65*, 1153–1163.

Vondenhof, A., Oslender, A., Deuticke, B., and Haest, C.W. (1994). Band 3, an accidental flippase for anionic phospholipids? Biochemistry *33*, 4517–4520.

Wang, C.C., Moriyama, R., Lombardo, C.R., and Low, P.S. (1995). Partial characterization of the cytoplasmic domain of human kidney band 3. J. Biol. Chem. *270*, 17892–17897.

Waugh, R.E., and Agre, P. (1988). Reductions of erythrocyte membrane viscoelastic coefficients reflect spectrin deficiencies in hereditary spherocytosis. J. Clin. Invest. *81*, 133–141.

Willardson, B.M., Thevenin, B.J.-M., Harrison, M.L., Kuster, W.M., Benson, M.D., and Low, P.S. (1989). Localization of the ankyrin binding site on erythrocyte membrane protein, band 3. J. Biol. Chem. *264*, 15893–15899.

Woods, C.M., Boyer, B., Vogt, P.K., and Lazarides, E. (1986). Control of erythroid differentiation: asynchronous expression of the anion transporter and the peripheral components of the membrane skeleton in AEV- and S13-transformed cells. J. Cell Biol. *103*, 1789–1798.

Zenke, M., Kahn, P., Disela, C., Vennström, B., Leutz, A., Keegan, K., Hayman, M.J., Choi, H.-R., Yew, N., Engel, J.D., and Beug, H. (1988). v-*erbA* specifically suppresses transcription of the avian erythrocyte anion transporter (band 3) gene. Cell *52*, 107–119.